PROCEEDINGS OF THE ROYAL SOCIETY A

FirstCite® e-publishing

Proc. R. Soc. A
doi:10.1098/rspa.2008.0024
Published online

Law of spreading of the crest of a breaking wave

By Y. Pomeau[1], T. Jamin[2], M. Le Bars[2,*], P. Le Gal[2] and B. Audoly[3]

[1]*Laboratoire de Physique Statistique, École Normale Supérieure, 24 rue Lhomond, 75231 Paris Cedex 05, France*
[2]*Institut de Recherche sur les Phénomènes Hors Équilibre, UMR 6594, CNRS and Aix-Marseille Université, 49 rue F. Joliot-Curie, BP146, 13384 Marseille Cedex 13, France*
[3]*Laboratoire de Modélisation en Mécanique, UMR 7607, Université Pierre et Marie Curie, 4 Place Jussieu, case 162, 75252 Paris Cedex 05, France*

In a wide range of conditions, ocean waves break. This can be seen as the manifestation of a singularity in the dynamics of the fluid surface, moving under the effect of the fluid motion underneath. We show that, at the onset of breaking, the wave crest expands in the spanwise direction as the square root of time. This is first derived from a theoretical analysis and then compared with experimental findings. The agreement is excellent.

Keywords: wave breaking; singularity; nonlinear hyperbolic equations

1. Introduction

Wave breaking in shallow water may be seen as the expression in the real world of the occurrence of a singularity in the solution of the equations of motion for a free surface. Somewhat related ideas have been presented by Whitham (1974), without, however, making predictions for the widening of the rolling crest. The wave breaking is a singularity because this set of equations is derived under the assumption that the surface is close to horizontal and because its solution after a finite time has a vertical tangent plane. This problem is studied first in a model, assumed to be generic for this type of singularity: the so-called Burger's equation. This yields generic scaling laws for various quantities near the singular time. Usually, the analysis of this model is limited to dependence with respect to one space coordinate and to time. This is not sufficient for the breaking of real waves involving deformations of a two-dimensional surface and therefore needing two space coordinates. Just after breaking this surface includes a closed non-planar curve where its tangent plane is vertical, this curve growing from a point at the onset of singularity. In a hypothetical two-dimensional world, the study of the one-dimensional Burger's equation would apply to the typical situation for wave breaking and the curve just mentioned would reduce itself to a pair of points.

* Author for correspondence (lebars@irphe.univ-mrs.fr).

Received 23 January 2008
Accepted 27 February 2008

In our three-dimensional world, the wave breaking occurs generically at a point on a surface and spreads later on in the spanwise direction. This paper gives the time dependence of this spreading. Real waves are described by highly nonlinear equations without hope of any explicit general solution. Therefore we rely on an analysis of the breakdown of smooth solutions of model equations with two space coordinates. In this model the width of the singular region increases generically like the square root of the time difference between the actual time and the instant where the solution becomes singular first. Then we show theoretically that the same breaking process occurs in 'real' water waves, in the approximation of long wave, relatively small amplitude and negligible dispersion. In the last part, we present experimental observations of the spreading of the crest of breaking waves in a laboratory set-up allowing accurate measurements in shallow water, showing a remarkable agreement with the theoretically predicted exponent.

2. From one-dimensional to two-dimensional wave breaking: a model

Below we first recall standard results on the so-called one-dimensional (1D) inviscid Burger's equation and extend them to two space dimensions. The main result of the two-dimensional analysis is that the width of the singular region grows like the square root of time, after the first singularity.

In 1808 Poisson explained how to solve the Cauchy problem for the equation

$$\frac{\partial u}{\partial t} + u\frac{\partial u}{\partial x} = 0. \tag{2.1}$$

Thanks to his solution it is possible to show the occurrence of singularities after a finite time for a wide class of smooth initial data. The equation (2.1) has the implicit solution

$$u(x, t) = u_0(x - ut), \tag{2.2}$$

where $u_0(x)$ is the initial condition, taken at $t=0$. Note that (i) in the following, we change the origin of time so that the first singularity in the solution of Burger's equation takes place at $t=0$ (the initial condition is then somewhere at $t<0$) and that (ii) we do not specify what this initial condition is (we only need it to be bell-shaped and smooth).

Another way of writing this solution is to consider the argument of u_0, on the r.h.s. of equation (2.2), as a function of $u(x, t)$

$$f(u(x,t)) = x - ut, \tag{2.3}$$

where $f(\cdot)$ is the inverse function of $u_0(\cdot)$. It is a classical result that for any bell-shaped and smooth initial data u_0, the first singularity of $u(x, t)$ appears at the inflection point of the function u_0 on the right of the maximum when u_0 is positive (figure 1).

Indeed, the singularity happens when the solution $u(x, t)$, as given by equation (2.3), becomes multi-valued, that is whenever $\partial x/\partial u=0$, the derivative is taken at constant t. This yields

$$t + \frac{\mathrm{d}f}{\mathrm{d}u} = 0. \tag{2.4}$$

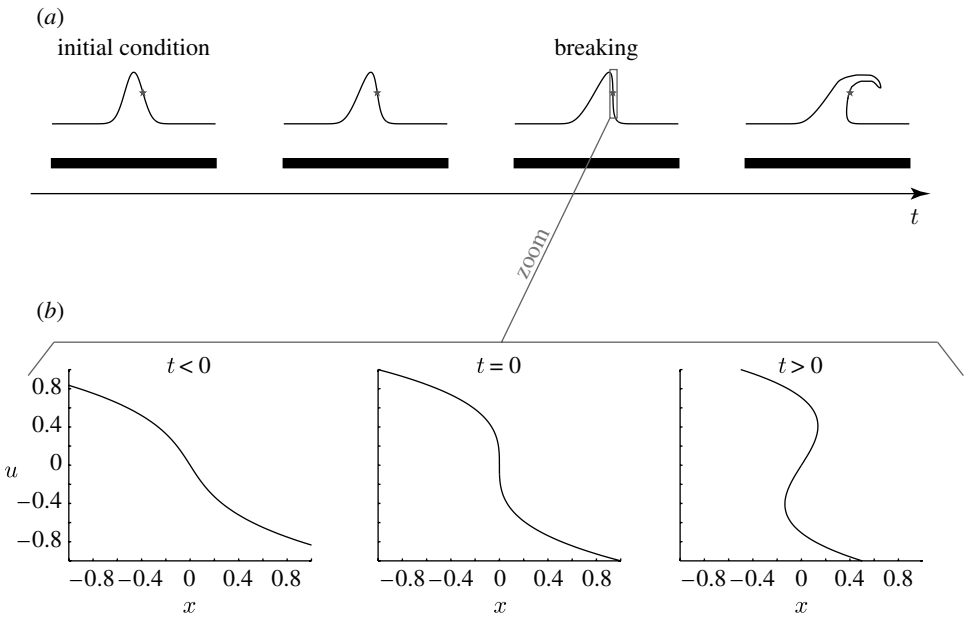

Figure 1. (*a*) Sketch of the typical time evolution of a one-dimensional breaking wave, starting for instance from a Gaussian profile. The star indicates the inflection point where the singularity first appears. (*b*) Resolution at three different times of the universal equation for the 'wave breaking' (2.5), valid at first order for any bell-shaped and smooth initial condition, considering that the first singularity takes place at $t=0$ and $x=0$ with $u=0$ (after changing the origins of time and space and after the Galilean transform).

For a given $f(u)$, the smallest time when equation (2.4) has a solution is when this solution is stationary with respect to t, that is, when $\mathrm{d}t=0$. Equation (2.4) then yields $0=\mathrm{d}t=-\mathrm{d}u(\mathrm{d}^2f/\mathrm{d}u^2)$ or simply $\mathrm{d}^2f/\mathrm{d}u^2=0$. Let us now look at the Taylor expansion of $f(u)$ around this point. Constant and linear terms can be eliminated by changing the origins of time and space and by the Galilean transform (i.e. the first singularity takes place at $t=0$ and $x=0$ with $u=0$). Therefore, the Taylor expansion of $f(u)$ reads $f(u)=-u^3+au^4+\cdots$, the coefficient of u^3 being negative to have a singularity appearing in forward times. Once put into equation (2.3), this gives at lower order the universal equation for the 'wave breaking', valid for any bell-shaped and smooth initial condition at $t_0<0$

$$0=u^3+x-ut. \tag{2.5}$$

For short times (i.e. around the breaking time $t=0$), u scales like $t^{1/2}$ and x like $t^{3/2}$, this making of the same order, $t^{3/2}$, all terms on the r.h.s. of equation (2.5).

Note that the result $u(x)$ of (2.5) is single valued for t negative and triple valued for t positive (figure 1). If a small dissipative term is added to the equation (2.1) to make it resemble the Navier–Stokes equation, one obtains the so-called Burger's equation

$$\frac{\partial u}{\partial t}+u\frac{\partial u}{\partial x}=\epsilon\frac{\partial^2 u}{\partial x^2}, \tag{2.6}$$

where ϵ is a small and positive coefficient. The addition of this dissipative term is a way of regularizing the solutions of (2.1), the multi-valued results being replaced by a jump around $x=0$, which represents a shock for this model.

The novelty of our study comes from the extension of this standard approach to the problem of formation of shocks in solutions of nonlinear hyperbolic equations with more than one space variable. Consider for instance the case of two space variables, x and y, and let $u(x, y, t)$ and $v(x, y, t)$ be the two Cartesian components of the velocity field. The generalization of the nonlinear equation (2.1) reads

$$\frac{\partial u}{\partial t} + u\frac{\partial u}{\partial x} + v\frac{\partial u}{\partial y} = 0 \tag{2.7}$$

and

$$\frac{\partial v}{\partial t} + u\frac{\partial v}{\partial x} + v\frac{\partial v}{\partial y} = 0. \tag{2.8}$$

This represents the 'fluid mechanics' equations for a gas without pressure, the origin of which can be traced back to the *Principia*, scholium, at the end of proposition IV, problem II, book 2, where Newton (1687) derives the quadratic law of drag for bodies moving in a fluid 'void of tenacity' in the words of the English translation by Motte (1729) (the newer translation by Cohen & Whitman (1999) translates the original Latin words into 'lacking in rigidity'). This set of equations has been used by Zel'dovich (1970) to explain the formation of large-scale structures in the Universe, assuming a potential flow. We now suggest that it provides a model for the occurrence of singularities for time-dependent functions of two space coordinates (x, y).

Similarly to the one-dimensional case, equations (2.7) and (2.8) admit a formal solution

$$x - tu(x, y, t) = F(u, v) \tag{2.9}$$

and

$$y - tv(x, y, t) = G(u, v), \tag{2.10}$$

where $F(u, v)$ and $G(u, v)$ are defined by the initial conditions. A crucial remark for the following is that the l.h.s. of the equations (2.9) and (2.10) are invariant under general transformations of the linear group. Let $\mathcal{M}$ be the general two-by-two matrix of this group, with non-zero determinant. It is obvious that $(\tilde{u}, \tilde{v}) = \mathcal{M}(u, v)$ and $(\tilde{x}, \tilde{y}) = \mathcal{M}(x, y)$ are solutions of equations of the same form as the l.h.s. of equations (2.9) and (2.10). This holds true with the *same* matrix $\mathcal{M}$ acting on (u, v) and (x, y). Of course the same general linear map will change in general the functions $F(u, v)$ and $G(u, v)$ in a rather complicated way, but because the map is linear, it will not change the degree of a polynomial in u and v. Thanks to this remark we shall be able to show, without calculation, that singularities yielding discontinuities of derivatives with respect to x may spread in any direction, the analysis being made by assuming first that the singularity spreads normal to x.

For smooth initial data, F and G are such that the initial mapping from (u, v) to (x, y) is one to one. The solutions of equations (2.7) and (2.8) become singular whenever the time-dependent Jacobian $J(t)$ of the mapping from (u, v) to (x, y) becomes singular at a certain time t. This Jacobian reads

$$J(t) = \left(\frac{\partial G}{\partial v} + t\right)\left(\frac{\partial F}{\partial u} + t\right) - \frac{\partial G}{\partial u}\frac{\partial F}{\partial v}. \tag{2.11}$$

Let us assume that the singularity occurs first at $t=0$ and at $x=y=0$ with $u=v=0$ too. As in the one-dimensional case, this last restriction is not as important as one could believe first: the original equations are Galilean invariant, so that one can always bring to $u=v=0$ the velocity field at some point of time and space. The condition equivalent to the cancellation of the second derivative of $f(u)$ at $u=0$ here is the property that, near $t=u=v=0$, the first non-vanishing terms in the Taylor expansion of the Jacobian $J(t)$ read

$$J(t) = at + bu^2 + cv^2 + 2duv + \cdots, \tag{2.12}$$

where a, b, c and d are constants derived from initial conditions. To give the quadratic term $(bu^2 + cv^2 + 2duv)$ in the Jacobian, $F(u, v)$ and $G(u, v)$ have to be expanded in Taylor series to third order, which depends on two sets of 10 coefficients. But the algebra is greatly simplified by limiting oneself to the leading-order terms near the singularity. Indeed, at $t=0$, the Jacobian matrix has a zero eigenvalue that can be associated to an eigenvector pointing in the x direction. Therefore the coefficients of the Taylor expansion of $F(u, v)$ and $G(u, v)$ are such that $\partial F/\partial u=0$, $\partial F/\partial v=0$ and $\partial G/\partial u=0$ at $u=v=0$. This yields that, near the singularity, the leading-order term in $F(u, v)$ and $G(u, v)$ should be

$$F(u, v) = b'v^2 + d'u^3 + g'uv^2 + f'u^2v \quad \text{and} \quad G(u, v) = c'v, \tag{2.13}$$

where the various coefficients can be easily related to b, c, and d through equation (2.12). Then, at leading order, equations (2.9) and (2.10) become

$$x - ut = b'v^2 + d'u^3 + g'uv^2 + f'u^2v, \tag{2.14}$$

$$y = c'v, \tag{2.15}$$

the term tv in (2.10) being negligible compared with $c'v$. Further simplifications of equation (2.14) are now possible. First, one can note that the term $b'v^2 = (b'/c'^2)y^2$ changes the support of the singularity from a straight line to a bent line without playing any other significant role: near the singularity one may always approximate the line of singularity by a straight line. Second, one can also neglect the term $f'u^2v = (f'/c')u^2y$, since it can be absorbed into a change of u into $u+ey$, e being a constant. After rescaling, equation (2.14) finally leads to a universal equation for the wave breaking in two space dimensions, valid for any bell-shaped and smooth initial conditions

$$0 = u^3 + x - u(t - y^2). \tag{2.16}$$

Note that all terms in equation (2.16) are of order $|t|^{3/2}$ near the singularity, with $y \sim |t|^{1/2}$, $u \sim |t|^{1/2}$ and $x \sim |t|^{3/2}$. This shows our main point, namely that the crest of the breaking wave (if this theory applies to the real phenomenon of wave breaking) spreads like $\sqrt{t}$ after the inception of the singularity, something that we will now verify in a real fluid mechanics configuration.

Let us end this section with three remarks.

(i) Note that x and y do not have to be coordinates along orthogonal axis, because the Jacobian matrix is reduced to its diagonal form by a general change of coordinates which is not necessarily a rotation, the Jacobian being not real symmetric in general.

(ii) Supposing that $u(x, y, t)$ behaves in the same way as the vertical position $z(x, y, t) = u(x, y, t)$ on the surface of a breaking wave (which is the case in shallow water, see §3), one finds the loci of points of vertical slope on the surface (the contour of the surface) by deriving from equation (2.16) the coordinates of the points where $dz=0$. The projection on the horizontal plane of this curve has Cartesian equation

$$27x^2 = 4(t-y^2)^3,$$

although the z coordinate is such that $z^2 = (t-y^2)/3$, the determination $z = \sqrt{(t-y^2)/3}$ being taken when x is positive and $z = -\sqrt{(t-y^2)/3}$ with x negative, all this because $x = 2u/3(t-y^2)$ and $t > y^2$.

(iii) In higher space dimensions, practically in three dimensions, the reasoning above still works, at least in its general lines. The first and most obvious situation is the onset of formation of a shock wave in a compressible gas (this shock wave could be generated by pushing impulsively a parabolic metal sheet in a gas, leading to the formation of a shock wave near the focus), supposing none exists before the critical time $t=0$. A simple extension of the arguments presented shows that the field $u(x, y, z, t)$, solution of the pressure-less Bernoulli equations, becomes singular at one point in the three-dimensional geometrical space and at a definite time, taken as zero. Locally this field is given by a root of the equation

$$0 = u^3 + x - u(t-y^2-z^2). \tag{2.17}$$

In this equation y and z are coordinates in a system of oblique axis depending on the initial conditions. In the physical three-dimensional space with the regularization by diffusion, the singularity is supported by an ellipse expanding homothetically with a size increasing as $\sqrt{t}$. This would be the case at the onset of formation of a generic shock wave in a compressible gas. But there is more than that in the above analysis. One can also study the case where the coefficient of u has signs different from the ones in equation (2.17). Consider what happens if this coefficient is $(t-y^2+z^2)$ instead of $(t-y^2-z^2)$. For any value of t the equation for u, namely $0 = u^3 + x - u(t-y^2+z^2)$, has three solutions, at least in certain domains of the (x, y, z) space, domains that collapse to a surface under the Maxwell construction, a surface making the shock wave. It means that there is a shock wave supported by a surface before and after $t=0$. The edge of the shock wave surface is where and when the coefficient of u is zero, which is along the hyperbola $t = y^2 - z^2$. At $t=0$ this hyperbola degenerates into its two straight asymptotes, $y = \pm z$. On a larger scale, there are one or two shock surfaces that may either merge to a single point or break in two pieces, depending on which side of the hyperbolae lies the shock. The local hyperbolae are the edges of the shock surface, the jump across the shock tending to zero as one moves along the shock surface towards this edge. A hard to read paper by Arnold *et al.* (1991) deals with a related topic, the bifurcations of a shock surface.

3. Wave breaking in shallow water

The analysis presented before does not apply directly to the case of real water waves, because they are not described mathematically by the equations for a fluid void of tenacity, or which is pressure-less. However it can be shown, as done below, that, in a well-defined limit, this theory is relevant for the breaking of waves in shallow water. This is done by estimating the typical quantities describing the wave breaking in a way inspired by the pressure-less case and by showing that, in a reference frame moving at the speed of linear waves, one recovers the equations of the pressure-less fluid near the singularity.

The dynamics of long waves in a layer of inviscid fluid of depth much smaller than the typical range of variation of the various quantities involved (see §4 for a discussion of the order of magnitudes involved) can be described by the following set of equations for the basic quantities corresponding to the fluid depth $h(x, y, t)$ and to the two Cartesian components of the horizontal fluid velocity, $u(x, y, t)$ and $v(x, y, t)$: the condition of mass conservation reads

$$\frac{\partial h}{\partial t} + \frac{\partial (uh)}{\partial x} + \frac{\partial (vh)}{\partial y} = 0, \tag{3.1}$$

the condition of momentum conservation in the x-direction reads

$$\frac{\partial u}{\partial t} + u\frac{\partial u}{\partial x} + v\frac{\partial u}{\partial y} + g\frac{\partial h}{\partial x} = 0 \tag{3.2}$$

and in the y-direction

$$\frac{\partial v}{\partial t} + u\frac{\partial v}{\partial x} + v\frac{\partial v}{\partial y} + g\frac{\partial h}{\partial y} = 0. \tag{3.3}$$

In equations (3.2) and (3.3), g is the positive acceleration of gravity. This set of equations admits non-trivial simple wave solutions whenever no function depends on y (for instance). Non-trivial solutions including both a dependence on x, y and t do not seem to exist. Nevertheless, it is possible to analyse the occurrence of singularities by solving this set in a convenient limit.

Let us do it first for solutions depending on x only. We assume that $h = h_0 + \tilde{h}(x, t)$, where h_0 is the constant (and positive) depth, much larger than the small perturbation $\tilde{h}(x, t)$. This allows to neglect terms of order $\tilde{h}(x, t)u$ with respect to $h_0 u(x, t)$. The new set of equations reads

$$\frac{\partial \tilde{h}}{\partial t} + u\frac{\partial \tilde{h}}{\partial x} + h_0\frac{\partial u}{\partial x} = 0 \tag{3.4}$$

and

$$\frac{\partial u}{\partial t} + u\frac{\partial u}{\partial x} + g\frac{\partial \tilde{h}}{\partial x} = 0. \tag{3.5}$$

Note that, although $\tilde{h}$ has been neglected with respect to h_0 in front of $\partial u/\partial x$, $u(\partial \tilde{h}/\partial x)$ has been kept, because it is *a priori* not smaller than any other term written explicitly in equation (3.4) (in particular, at the singularity, we expect the x derivative to go to infinity).

Take now h_0 as unit for $\tilde{h}$, introduce C_{B} such that $C_{\mathrm{B}}^2 = gh_0$ (the subscript B is to recall that this velocity was derived first by Bernoulli), take C_{B} as unit for u and choose new units for t and x such that their ratio is 1 when their ratio in

physical units is C_{B}, the equations for $\tilde{h}$ and u become

$$\frac{\partial \tilde{h}}{\partial t} + u\frac{\partial \tilde{h}}{\partial x} + \frac{\partial u}{\partial x} = 0 \tag{3.6}$$

and

$$\frac{\partial u}{\partial t} + u\frac{\partial u}{\partial x} + \frac{\partial \tilde{h}}{\partial x} = 0. \tag{3.7}$$

Those equations become identical if $u = \tilde{h}$. This corresponds to the so-called simple wave. Let $u = \tilde{h} = w$, the two equations (3.6) and (3.7) become the single one

$$\frac{\partial w}{\partial t} + w\frac{\partial w}{\partial x} + \frac{\partial w}{\partial x} = 0. \tag{3.8}$$

This is brought back to the familiar (so-called) inviscid Burger's equation (2.1) by the change of unknown function from w to $(w+1)$. It shows that the singularity is the same as the one found before, of course not a new result at all, owing to the possibility of solving the full set (3.1)–(3.3) by Riemann's method with $v=0$ and no dependence on y.

Let us now look at the dimensionless equations for the nonlinear wave propagation in shallow water in two space dimensions, using the same scaling. The mass conservation yields

$$\frac{\partial \tilde{h}}{\partial t} + \left(\frac{\partial u}{\partial x} + \frac{\partial v}{\partial y}\right) + u\frac{\partial \tilde{h}}{\partial x} + v\frac{\partial \tilde{h}}{\partial y} = 0. \tag{3.9}$$

The conditions of momentum conservation along x and y read

$$\frac{\partial u}{\partial t} + u\frac{\partial u}{\partial x} + v\frac{\partial u}{\partial y} + \frac{\partial \tilde{h}}{\partial x} = 0 \tag{3.10}$$

and

$$\frac{\partial v}{\partial t} + u\frac{\partial v}{\partial x} + v\frac{\partial v}{\partial y} + \frac{\partial \tilde{h}}{\partial y} = 0. \tag{3.11}$$

Let us assume first that the scaling laws for y, x, t and u are the same as in the generic singularity of the two-dimensional Burger's equation, that is $y \sim |t|^{1/2}$, $x \sim |t|^{3/2}$ and $u \sim v \sim |t|^{1/2}$. Then in equation (3.9), $(\partial u/\partial x) \sim |t|^{-1}$ is dominant compared with $(\partial v/\partial y) \sim |t|^{0}$. Therefore at leading order, equation (3.9) becomes

$$\frac{\partial \tilde{h}}{\partial t} + \frac{\partial u}{\partial x} + u\frac{\partial \tilde{h}}{\partial x} + v\frac{\partial \tilde{h}}{\partial y} = 0.$$

Similarly to the one-dimensional case, we can then look for a simple wave solution, i.e. $\tilde{h} = u$. Taking $w = u+1$ as new unknown function, one finds that (3.9) and (3.10) reduce to a single equation for w

$$\frac{\partial w}{\partial t} + w\frac{\partial w}{\partial x} + v\frac{\partial w}{\partial y} = 0.$$

Let us now write equation (3.11) with this new function w

$$\frac{\partial v}{\partial t} + w\frac{\partial v}{\partial x} + v\frac{\partial v}{\partial y} - \frac{\partial v}{\partial x} + \frac{\partial w}{\partial y} = 0.$$

The first three terms correspond to the two-dimensional Burger's equation, whereas the last two terms correspond to the vertical vorticity. Let us look at their contribution, assuming that the scaling from §2 holds: $\partial v/\partial x$ is then zero, whereas $\partial w/\partial y$ induces a negligible correction on v of order t. This means that starting from an irrotational initial condition (a smooth wave propagating in the x direction with no y dependence), no vorticity generation is to be expected at the first order relevant to our theory. Note, however, that this does not preclude vorticity generation at higher order at the edge of the breaking zone, as shown for instance by Peregrine (1999) at the edge of bores. This very interesting question is beyond the scope of the present paper, but will be the focus of future theoretical and experimental studies.

Neglecting the vorticity, the system to be solved is the same as the one solved for the pressure-less fluid. This proves our point, namely that at leading order the singular solution is for $u(\cdot)$ (and so for $\tilde{h}$) the same as for the pressure-less case, up to the addition of the constant speed necessary to get rid of the Galilean change of frame of reference, the fluid velocity v being just proportional to y. In particular, the widening of the wave-breaking domain in the y direction scales like the square root of time.

The calculation above suggests that this behaviour is 'universal' for nonlinear non-dispersive waves. Other kind of waves are known to break, such as the ocean waves on deep water (with, practically, infinite depth) or the gravity waves in the atmosphere. Does their spreading in the y direction follow the same square root law? The answer to this question depends in particular on how precise can be set the instant of time of the breaking process.

4. Wave breaking in the one-dimensional case: nonlinearity versus dispersion

This section is to look more closely at the wave breaking in one dimension. More specifically, we make the connection between the solution of the equations (3.1)–(3.3) and the real wave breaking. The need to do this arises from the simple observation that the long-wave equations are clearly invalid at the time of the break-up and presumably some time before because the slope $\partial h/\partial x$ then diverges, although the equations are derived under the assumption of a surface with a small slope. This situation is rather common in many problems where the onset of singularity is just a witness that somewhere and sometime another approximation (or another method) has to be used to solve the problem at hand, an approximation different from the one that leads to the singular behaviour.

It is known that dispersion effects occurring at the next order in the shallow water approximation (the small parameter being the fluid depth and the leading order the equations of the previous section) yield the Korteweg–de Vries (KdV) equation in the co-moving frame. The KdV equation has no finite time singularity with smooth initial data and yields instead solitons where the nonlinearity and the dispersion balance each other to avoid singularities. It is worth pointing out that this discussion is a very natural extension of the one made long ago by Stokes to define precisely the range of validity of the linearized Boussinesq theory. It is at least in qualitative agreement with the observation reported in §5 that waves break or not depending on their amplitude: at small amplitude dispersion dominates and there is no breaking, although at higher amplitudes nonlinear effects dominate and waves break.

The KdV equation in the frame of reference moving with the speed of the waves in the linear approximation, that is $C_{\mathrm{B}} = \sqrt{gh_0}$, reads

$$\frac{\partial \tilde{h}}{\partial t} + A\tilde{h}\frac{\partial \tilde{h}}{\partial x} + B\frac{\partial^3 \tilde{h}}{\partial x^3} = 0, \tag{4.1}$$

where $A = C_{\mathrm{B}}/h_0$ and B is proportional to $C_{\mathrm{B}}h_0^2$ with a numerical constant irrelevant for this discussion. This equation applies if the nonlinear and regularizing terms are of the same order of magnitude, which requires

$$\frac{\tilde{h}}{h_0} \sim \left(\frac{h_0}{\Lambda}\right)^2,$$

where Λ is the typical length scale for the variation with respect to x, although the amplitude of $\tilde{h}$ is denoted simply as $\tilde{h}$. If on the contrary

$$\frac{\tilde{h}}{h_0} \gg \left(\frac{h_0}{\Lambda}\right)^2,$$

the nonlinearities dominate the effects of dispersion, and wave breaking occurs with suitable initial conditions, as demonstrated theoretically in the previous section and as will be seen experimentally in the next section. Note finally that the opposite condition was found by Stokes (1847) for the applicability of the linear approximation for waves propagating in shallow water.

Near the singularity the slope of the surface will diverge so that the long-wave equations are clearly invalid in an inner region. The order of magnitude of the (inner) domain where the shallow water approximation does not apply is found by writing the equation (2.5) with physical quantities relevant for the wave-breaking problem. The inner region is the neighbourhood of $x = t = 0$, where the slope $\mathrm{d}h/\mathrm{d}x$ becomes of order 1. The equation $f(u) = -u^3$ becomes in physical units $f(u) = -\alpha u^3$ with $\alpha = (\Lambda/C_{\mathrm{B}}^3)(h_0/\tilde{h})^3$. This scaling law is derived by noticing that, near the singularity, $\tilde{h}(x) \sim \tilde{h}(x/\Lambda)^{1/3}$ and that $u \sim (C_{\mathrm{B}}/h_0)\tilde{h}$. With the scaling laws derived in §2, one finds that if $(\mathrm{d}h/\mathrm{d}x) \sim 1$, then $t \sim t^*$ with $t^* = h_0/C_{\mathrm{B}}$. From the scaling $x \sim t^{3/2}\alpha^{-1/2}$, the width of the inner region is $x^* \sim \tilde{h}^{3/2}/\Lambda^{1/2}$. Indeed the scaling laws just derived are only valid until the time of break-up, where another approximation has to be used. In the wave-breaking problem, one expects regularization (something allowing practically to describe what happens beyond the singularity occurring in the shallow water approximation) by taking into account the complete fluid equations instead of their long-wave limit. This regularization changes the local equations near the area where overturning occurs, but it does not change the scaling laws for the extent of this area in time and space. This regularization is purely local, although the large scales remain described by the long-wave approximation, making the outer problem. The resulting multi-scale analysis will be presented in a future publication.

5. Experimental validation: breaking waves in shallow water

The above theory has been checked against experiments measuring the spanwise widening of the breaking of a wave in shallow water. The experiments were realized on a 2 m long and 1.4 m wide water table. Figure 2 shows this table with

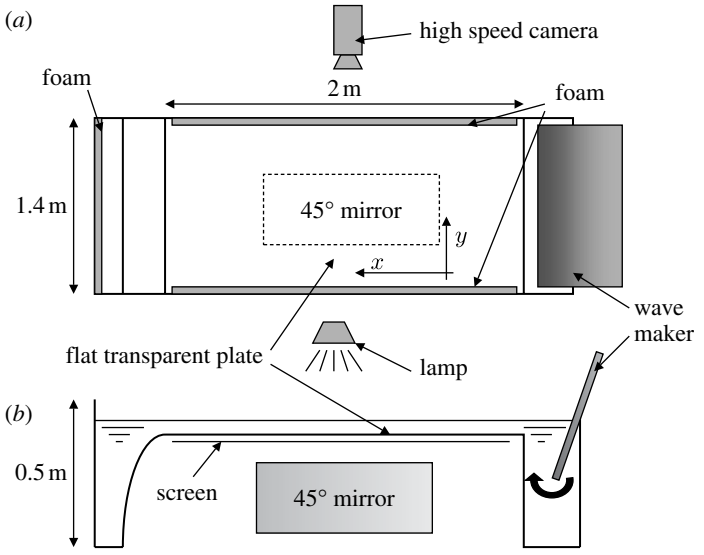

Figure 2. Experimental set-up, (*a*) top view and (*b*) side view. A solitary wave is generated by the rapid motion of the wave maker on one side of a water table. The surface deformations, travelling along the longitudinal x direction, are visualized by shadowgraphy and recorded by a high-speed camera.

its two water tanks and its transparent glass bottom. The level h_0 of water above the bottom is adjusted to reach the desired values (between 1 and 2 cm). The waves are generated by the motion of a rectangular plate (the wave maker), which is partially immersed in one of the tanks at the end of the table. The controlled motion of this thick PVC plate around a horizontal axis pushes a certain amount of water and so generates a solitary wave that propagates along the table. On a large scale, this wave is close to being straight and perpendicular to its direction of motion. The swing motion of the wave maker is simply induced by its own weight. The generated wave may break or not depending of its height compared with the water depth. The experimental parameters are then adjusted to make the wave break in the centre of the working area on the table. To suppress as much as possible reflections of waves on the vertical side walls, long stripes of plastic foam have been put on the water surface all around the inner walls of the table. To get reproducible waves and consequently a reproducible longitudinal location for the breaking, the starting position of the wave maker is measured accurately thanks to an optical positioning device and the ending position is fixed by two ropes attached to each side of the plate, their length being adjusted to stop the plate motion at the desired value. Underneath the bottom plate made of glass, a translucent screen permits the observation by shadowgraphy of the propagating wave and its breaking. A light projector is mounted 1.5 m above the table and it forms a shadowgraphic image of the deformed water surface on the screen. A mirror inclined at 45° allows to observe and record the phenomena occurring inside a square of approximately $32.5 \times 32.5\,\mathrm{cm}^2$. A high-speed camera with a rate up to 2.8 kHz records the waves and their breaking as they move along the table. The optical quality of the system was checked and calibrated by taking the image of a fixed grid.

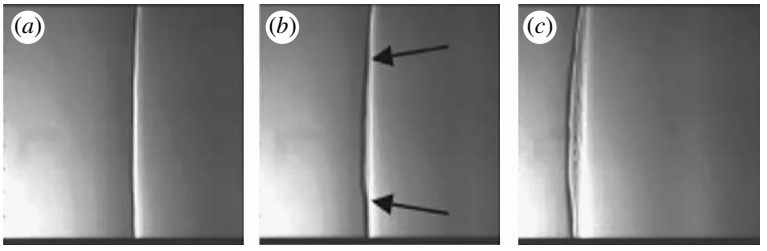

Figure 3. Shadowgraph of a wave breaking recorded by a high-speed camera. (*a*) $t=25$ ms, (*b*) $t=100$ ms, (*c*) $t=250$ ms. The arrows indicate the location of the singularities that progress along the transverse direction y. The size of the observation window is 32.5×32.5 cm^2.

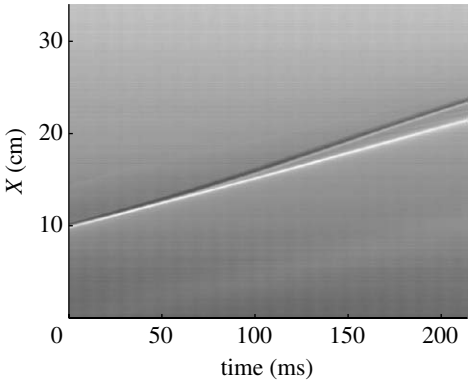

Figure 4. Space–time diagram illustrating the progression of the wave along x at a constant speed $v=0.41$ m s$^{-1}\sim\sqrt{gh_0}$ (white line) and the appearance of the wave breaking (black bent line). Water depth h_0 is 17.4 mm and wave height is 8 mm.

Experiments were made with five different depths: 15.5, 17.4, 19.7, and 22.5 mm. For each depth, 10 runs were performed and recorded. Each experiment corresponds to a different wave height that is measured at the beginning of each run by the use of a sheet of sandpaper held vertically and perpendicular to the wave. This is a simple and easy way to determine quite precisely (precision is approximately the size of the grains of the sandpaper) the height of the water waves, which was equal to respectively 6.3, 8.0, 10.6 and 9.3 mm for the previously given water depths. The longitudinal extent of the surface deformation is approximately 5 cm. These values justify the different approximations of the theoretical study presented in this paper (long wave—relatively small amplitude—negligible dispersion, i.e. $(h_0/\Lambda)^2<\tilde{h}/h_0<1$, see §4). Note also that these values fully justify to neglect the effects of viscosity and surface tension. Considering the typical viscosity of water (i.e. 10^{-6} m^2 s^{-1}) and the typical duration of one experiment (i.e. 0.3 s), the relevant viscous length scale is 5.5×10^{-4} m, much smaller than the typical wave size. Similarly, considering the surface tension of water (i.e. 0.073 N m^{-1}), the typical capillary length is approximately 2.7×10^{-3} m, much smaller than the typical wavelength.

Figure 3 shows an example of three consecutive images of a wave travelling from right to left. These images are taken from a high-speed movie recorded at a rate of 2.8 kHz. The vertical and the horizontal sizes of the visualization window are given by the size of the mirror. The wave appears as the juxtaposition of a white line and

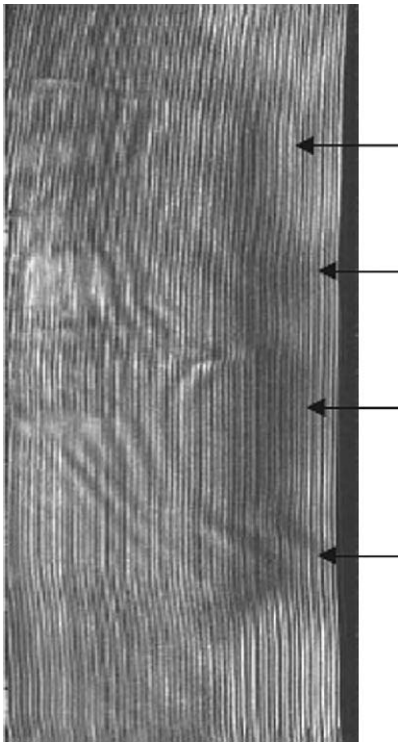

Figure 5. Superimposition of images separated by 5 ms and showing the progression of the wave (enhanced by taking the horizontal gradient) that appears as vertical stripes. The wave breaking appears as a black shadow, mainly concentrated at the centre of the figure. Time is proportional to the longitudinal coordinate and runs from right to left along the horizontal axis. Several sources of breaking are indicated by arrows before they merge.

a black line owing to the focusing of light by the wave crest and its defocusing in the trough. The breaking of the wave is clearly visible on images (*b*) and (*c*) by the bending of the black line travelling ahead of the straight part of the wave with a slightly larger speed. The arrows of figure 3*b* point the location of the two singularities propagating along the transversal direction y. Therefore the two lines separate in time, at least for the short durations of observation after the breaking started.

The longitudinal progression of the waves and that of their breaking can also be particularly well illustrated by performing space–time diagrams. Taking a horizontal line (corresponding to a given lateral position y) of each image and gathering the lines to reconstitute an image illustrate the progression of the wave along the table. Figure 4 shows an example of such a space–time diagram where both the travelling wave and its breaking are visible. The white line represents the wave crest and rear face progression along the x-axis. As the height of the wave is constant on the distance it travels along the longitudinal coordinate x, it is not surprising to recover the constant gravitational wave speed $C_{\mathrm{B}} = 0.41\ \mathrm{m\,s^{-1}} \sim \sqrt{gh_0}$ (the expected theoretical velocity is $C_{\mathrm{B}} = 0.46\ \mathrm{m\,s^{-1}}$). On the contrary, the black line that is the trace of the breaking during its progression along the table is slightly bent showing an acceleration of the breaking front ahead of the rest of the wave.

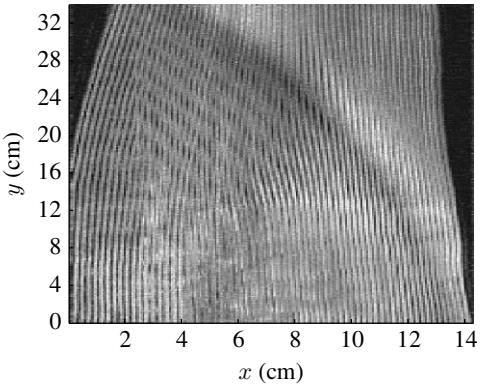

Figure 6. Wave-breaking trace as it progresses laterally towards the wall. Superimposition of images separated by 3 ms. Horizontal axis is proportional to time that runs from right to left. The depth of the water is 17.4 mm and the height of the wave is 8 mm.

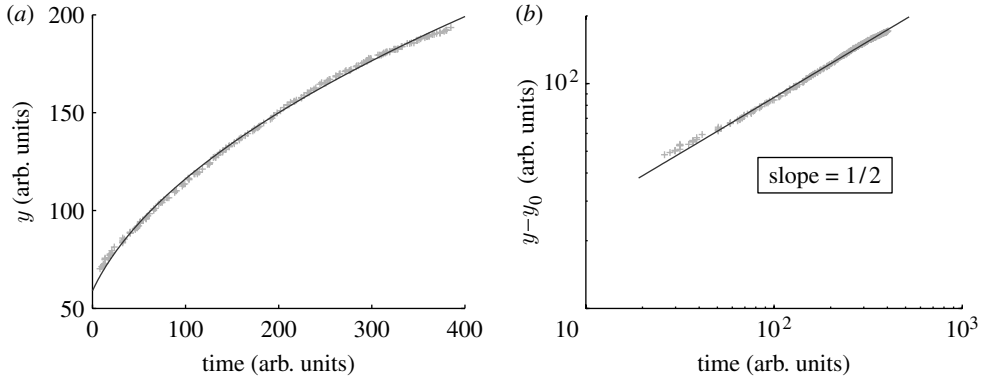

Figure 7. (*a*) Linear and (*b*) logarithmic representation of the progression in the time of the singularity along the lateral y-axis. The solid curve is a second-order fit of the experimental data points.

As may be seen by close inspection of figure 3, the breaking is initiated in the central region of the wave, far from the sidewall. We can then superimpose a complete series of images: as the wave travels at a constant speed, the longitudinal coordinate x is then directly proportional to time. To increase the contrast of the result, the horizontal gradient of each image is taken. Figure 5 presents this superimposition where successive images are separated by a time delay of 5 ms. It shows the progression of the wave from right to left at constant speed. The traces left by the wave appear as vertical stripes. The wave breaking appears as a black shadow, initiated at the centre of the figure. As can be observed, several sources of breaking appear and progress laterally in time before merging to form a unique breaking front. To study the lateral progression of one breaking, and thus of the associated singularities, we focus on one side of the wave which is at the top of the images. For that, the mirror is simply moved from the centre of the table to one side. Following the same image analysis as before, we record precisely the trace of the breaking waves that progress laterally. Figure 6 presents an example of the superimposition of images separated by 3 ms. The position of the shadow is easily determined visually. It gives a curve that represents the lateral progression

in time of the singularity associated with the breaking along the spanwise direction y (figure 7*a*). As can be observed in figures 6 and 7*a*, the shape of this curve is by simple inspection very close to a square root and finally, after having determined the initial position y_0 of the breaking, a log–log representation of this curve is given in figure 7*b* and clearly confirms the square root nature of the lateral progression of the singularity as predicted in §3.

A systematic image analysis of our 50 cases of waves shows that this behaviour, illustrated here on a single event, is truly generic: the breaking of the wave always progresses as the square root of time in the spanwise direction. We have also checked that the presence of a slight positive or negative slope (the table can be tilted by a few degrees in the longitudinal direction) has no significant effect on this behaviour. However, even if all waves break systematically with the expected square root behaviour, we have not found a clear evolution of the values of the coefficient γ ($y - y_0 = \gamma\sqrt{t}$) as functions of the wave height and/or the water depth. This coefficient depends on the initial conditions for the wave, depending on the uncontrolled small perturbations of the wave crest. It could be also that the range of variations of water depth and wave height in our set-up was too limited to permit a significant change in the coefficient of the square root law.

6. Summary and conclusion

A generic analysis of wave breaking predicts a widening of the crest with the square root of time after break-up begins. This is based on the general solution of the equations for a pressure-less inviscid fluid and can be extended, at least near the break-up, to the fluid equations for a long wave of relatively small amplitude and negligible dispersion. Experiments carried in a shallow horizontal fluid layer show this square root law for the breaking of solitary waves excited by a simple device. Therefore wave breaking can be seen as belonging to the general class of phenomena described by nonlinear hyperbolic equations, realizing somehow the prediction made long ago by Riemann who viewed his solution of the equations of compressible gases more as a piece of mathematics than as something related to the reality of gases. As we know, he was wrong in this respect, because shock waves do exist in compressible gases, but his discovery has truly a wider range of application, in particular to waves in shallow water as we show here. This has been known for a long time of course, but as far as we are aware no prediction has been made for the widening of the crest of a wave. We believe that this provides an interesting domain of investigation because there the regularization (i.e. what happens *after* the singularity) is quite different from the one in the much studied cases of regularization by dispersion or by diffusion, the latter being relevant for shock waves in gases.

References

Arnold, V. I., Baryshnikov, Y. M. & Bogaevsky, I. A. 1991 Singularities and bifurcations of potential flows. In *Nonlinear random waves and turbulence in nondispersive media*, Suppl. 2 (eds S. N. Gurbatov, A. N. Malakhov & A. I. Saichev). Manchester, UK; New York, NY: Manchester University Press.

Newton, I. 1687 *The mathematical principles of natural philosophy.* (Transl. Andrew Motte, London, 1729, and a new translation by Cohen, I. B. & Whitman, A. 1999 *The principia: mathematical principles of natural philosophy Isaac Newton.* Berkeley, CA: London, UK: University of California Press.)

Peregrine, D. H. 1999 Large-scale vorticity generation by breakers in shallow and deep water. *Eur. J. Mech. B* **18**, 403–408. (doi:10.1016/S0997-7546(99)80037-5)

Poisson S. D. 1808 Mémoire sur la théorie du son. *J. de l'École Polytechnique*, 14éme cahier **7**, 319–392. A short historical account of researches on the mathematical problem of generation of singularities in 1D nonlinear hyperbolic equations is to be found in Courant, R. & Friedrichs, K. O. 1967 *Supersonic flows and shock waves*, ch. III, pp. 118–119. New York, NY: Interscience Publishers.

Stokes, G. 1847 On the theory of oscillatory waves. *Camb. Phil. Trans.* **8**, 441–473.

Whitham, G. 1974 *Linear and nonlinear waves.* New York, NY: Wiley. Section 13.14.

Zel'dovich, Y. B. 1970 Fragmentation of a homogeneous medium through gravitation. *Astrophysics* **6**, 319–335.